

Target Detection Using Matched Filtering Analysis of the ASTER Data for Exploration of Uranium Mineralization in the Northern Part of El-Erediya Pluton, Central Eastern Desert, Egypt.

El Zalaky and Abdelmonsif

"Nuclear Materials Authority (NMA), P.O. Box 530 Maadi, Cairo, Egypt"
corresponding Email: melzalaky@gmail.com

Abstract

The younger granite of El-Erediya pluton represents one of the most important prospect areas in the Egyptian Central Eastern Desert which comprise surface and subsurface U-mineralization confined to the southern part of the pluton. Due to the high uranium airborne anomaly of the northern part than the southern part of the pluton, the granite of northern part need to reevaluate its U-potentiality according to the modern techniques that were developed in the last decade.

The main goal of this paper is to examine the efficiency of the Advanced Space-borne Thermal Emission and Reflectance Radiometer (ASTER) data in mapping the alteration zones that could be host uranium mineralization within the younger granite of El-Erediya pluton using spectral analysis techniques.

ASTER data are especially attractive to many geological researchers in Africa, due to their open availability and associated minimal costs for academic use. The three visible and six near-infrared bands, which have 15-m and 30-m resolution, respectively, were calibrated by using atmospheric correction.

Target detection using spectral-matching algorithm was applied to recognize the most predominant alteration components such as hematite, kaolinite, illite and alunite as more or less considered as path finder of uranium mineralization to trace the most promising zones affected by these alteration within the granite of El Erediya pluton.

Three ASTER-derived promising areas have been detected, including the prospect area, using the matched filtering methods with a confidence ranging from 68 to 95%. All of these zones that delineated by target detection technique show good correlation with those on field and on the reference geologic map.

Two of these target zones are proved in the field and founded along the structural features cutting the northern parts of El Erediya pluton that have not been identified before. Mineralogical studies were carried out, using ore and scanning microscope and XRD, for some selective mineralized samples collected from one of these two target zones. These investigations confirm the presence of uranophane mineral as uranyl silicates in addition to zircon and fluorite. These minerals are found in close association with hematitization, kaolinization, and illitization alteration.

Keywords: *Remote sensing, target detection, uranium, granite.*

1. Introduction

El-Erediya area is located in the Central Eastern Desert, at about 35 km to the south of road sign 85 km along the Qena-Safaga main road. El Erediya granite is an elongated oval shaped pluton in a NNW-SSE direction, with length of about 6.5 km and width of about 2.5 km. It forms one of the prominent topographic features in the area due to its resistance to the erosion, where it has a triangulation point reaching 983m absolute elevation above the sea level (a.s.l).

The study area has been subjected to detailed geological studies by many authors among them (Ammar1973, El-Kassas1974, Bakhite1978, Attawiya1983, Kamel1998, Abd El-Naby 2007 and others). These studies gave an understanding of the geology of the studied area.

Air-borne gamma-ray spectrometry data (Aero-Service, (1984) of the studied area showed that syenogranites of G. El-Erediya pluton have the highest radioactivity especially at the northern part of the pluton (Fig.1) which motivate the writers to find relation between the airborne gamma-ray and ASTER (VNIR-SWIR) spectral.

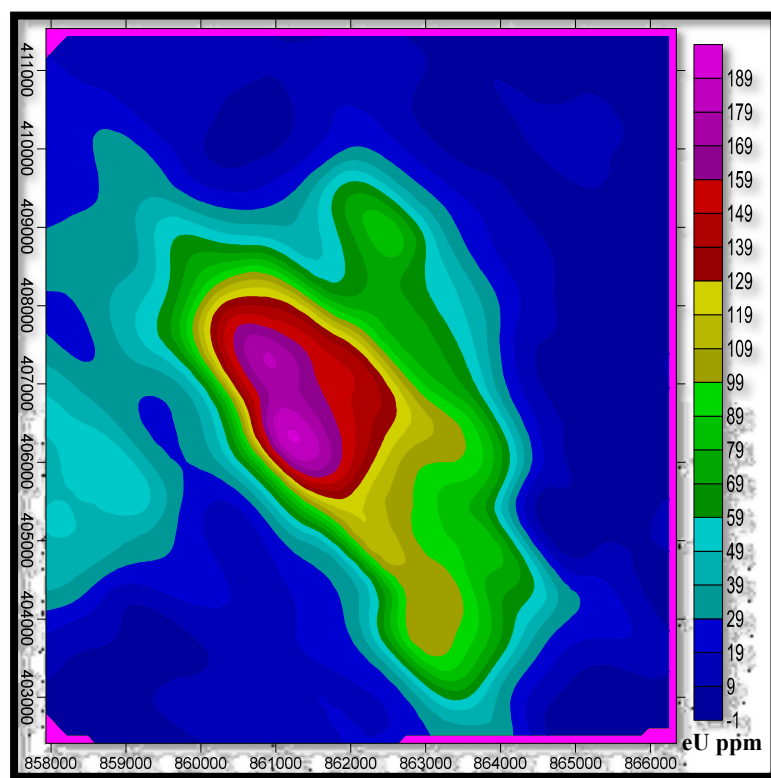


Fig.1: Filled color contour map of eU of El-Erediya pluton (Red Belt Projection).

The present study aims to link the previous valuable geological studies with the Remote Sensing Techniques to establish the common characteristic features leading to the recognition of more uranium mineralizations within El-Erediya granite as one of the most promising examples for the radioactive mineralizations among the Pan-African younger granites of the Eastern Desert of Egypt.

Remote sensing technology plays a vital role in the initial stages of ore deposits exploration especially in arid and semi-arid regions. Recognizing hydrothermally altered rocks through remote sensing instruments have been widely and successfully used for the exploration of epithermal ore deposits (Sabins, 1999, Tommaso and Rubinstein 2007, Zhang et al 2007, Amer et.al 2010, Azizi et.al 2010, Gabr et al 2010, Bedini, 2011, Pour and Hashim, 2011a).

In the past 15 years, new space borne multispectral and hyperspectral remote sensing instruments have been launched and have provided higher spectral resolution data that can be used for mineral exploration. In addition, the availability of laboratory-measured spectral data for rocks and minerals complements remote spectral measurements and allows geologists to identify unique lithologies (e.g. JPL, USGS, and ASU spectral libraries). These recent developments have enabled remote sensing technology to become an increasingly and powerful tool for mineral exploration, particularly for remote areas with little or no access.

The (ASTER) on NASA's Terra platform provides such measurements and has been widely used in geological and other studies (Rowan et al 2003, Hellman & Ramsey 2004, Hubbard & Crowley 2005, Ducart et al 2006, Zhang et al 2007, Rockwell & Hofstra, 2008, Vaughan et al 2005, 2008). ASTER is a multispectral imager, which provides observations in the visible and near infrared (VNIR, 0.4–1.0 μm), the short wavelength infrared (SWIR, 1.0–2.4 μm) and the thermal infrared (TIR, 8–12 μm) parts of the electromagnetic spectrum (Table 1).

Table 1. Characteristics of the ASTER sub-sensor system (Yamaguchi et al., 1998)

Subsystem	Band No.	Spectral range (μm)	Spatial resolution (m)	Signal quantization (bits)
VNIR	1	0.52–0.60	15	8
	2	0.63–0.69		
	3	0.78–0.86		
SWIR	3N	0.78–0.86	30	8
	4	1.60–1.70		
	5	2.145–2.185		
	6	2.185–2.225		
	7	2.235–2.285		
	8	2.295–2.365		
TIR	9	2.360–2.430	90	12
	10	8.125–8.475		
	11	8.475–8.825		
	12	8.925–9.275		
	13	10.25–10.95		
	14	10.95–11.65		

The (ASTER) data have been chosen in this study due to its availability and relatively good spectral (14 bands) and spatial resolution; so, it will be suitable in mapping the rock alteration zones especially by using the six short wave infrared (SWIR) bands.

The objective of this paper is to employ spectral image processing techniques that have been used often to process hyperspectral data (target detection) to analyze ASTER data for the purpose of mapping altered rocks, with the hope that these techniques will make effective use of the richer information content furnished by ASTER's relatively high spectral resolution. To achieve this, we have masked all the rock units surrounding the granite of El Erediya before applying the spectral analysis. The following section is devoted to introducing the regional setting of the area comprising El-Erediya granite, followed by a description of the ASTER sensor system and the remote sensing dataset used in this research. The spectral image analysis techniques applied to the ASTER dataset are then explained and the results are described. Finally, these results are discussed in terms of their geological implications.

2. Geological Setting

The rock units in the studied area are representing from the oldest to the youngest by metavolcanics, amphibolites, younger granites and wadi deposits. Several dykes and veins represented by aplites, porphyries, pegmatite and jasper as well as few basaltic dykes are represented in the area (Fig.2).

The granite of El-Erediya pluton is massive with pink color and medium to coarse grained and classified as syenogranite. This granite is surrounded by metavolcanic which is characterized by fine to medium grained, dark greenish to greenish black in color and dissected by the granite as offshoots or roof-pendants and xenoliths.

Amphibolites are medium to coarse grained with green to grayish green colors and intruded by a large number of aplite dikes and offshoots of granite, also, amphibolites occur as roof-pendants carried on the granite. On the other hand, there is no radioactivity in both metavolcanics and amphibolites.

Several types of dykes cut through El Erediya granite in several directions, these dykes are different in composition and represented by aplite, porphyries and basaltic ones. These dykes are poor in radioactivity except aplite dyke which record about 100 ppm eU.

Many pegmatite bodies of azoned and zoned pegmatite are spreading in El-Erediya granite with low radioactive content. El-Erediya granite has many shear zones especially in the southern part

of the pluton which has the mine of NW trend and other shear zones with NE-SW trend. These shear zones are found associated with jasper veins and some alteration features which record the highest values of radioactivity range from 100 to 5000 ppm eU in some shear zones.

El Erediya granite is affected by different types of alterations which are seen along the walls of the shear zones. These alterations are represented by hematitization (Fig.3a), silicification, kaolinization (Fig.3b), illitization specially in El-Missikate granite (Fig.3c) as well as subordinate sericitization and argillic alteration. Jasper is commonly developed as fracture fillings, associated with hematitization and limonitization and presence of visible uranium mineralizations (mainly uranophane).

Exploratory tunnels at southern part of the pluton and a core drilling program revealed that the mineralized fracture zones within the younger granite are extend downward below the wadi level. The reevaluate U-potentiality of these granitic types according to the modern theories were developed in the last decade.

El-Erediya granite is believed to be emplaced by the end of late Precambrian. The reported Rb-Sr age for El-Erediya granite is 570 Ma (Fullagar, 1980) and U-Pb age is about 583 Ma (Abu Deif, 1992). The uranium mineralization of El Erediya pluton is represented by uraninite as a primary uranium mineral while the secondary uranium minerals existing as uranophane, soddyite and renardite (Attawiyah, 1983) El-Erediya and El-Missikat granitic plutons along with the associating uranium mineralization were derived from a mantle source enriched in incompatible elements or there was a significant crustal involvement in their magma generation, also, they are anorogenic granites originated in a within plate environment and the uranium mineralization in both plutons is suggested to be formed from convection system during post- magmatic hydrothermal activity (Hussein, 1987). Pink granites in El-Erediya and El-Missikat have been subjected to more than one alteration process including silicification, argillic alteration, sericitization and ferrugination beside chloritization and carbonitization. On the other hand, the uranium minerals might have been leached from the surrounding granitic rocks under the action of meteoric water which heated after that by magmatic intrusions (Mohamed, 1988). The existence of five sets of fault zones striking N, NE, NW, NNE and WNW were provided and the N, NE and NW trends were found to represent ancient (deep-seated) as well as recent (near-surface) structures but the NNE and WNW trends were found to represent only recent structures, the main two maximum principle stresses are found to be oriented in E and NNE (Rabie and Ammar, 1990). There are at least four successive tectonic events that were alternated with magmatic activity and hydrothermal mineralization, the uranium mineralization belongs to the third tectonic event (of late Mesozoic to early Tertiary age) which is associated with rejuvenation, brecciation along NE to ENE faults, fractures systems and silica veins carrying the uranium minerals (Abu-Dief, 1992). The secondary uranium minerals at the Central Eastern Desert of Egypt were formed during the period 15000 to 60000 years ago and that the labile uranium in the adjacent rocks was adsorbed after that time (Osmand et al. 1999). Four locations of high radioactive anomalies with some uranium mineralization were discovered. Two of which are located at the western and northwestern parts of G. El Missikat granite, the third at the northern part of El Erediya pluton and the fourth at the northern part of G. Gatter at Wadi Mayet El Abd. The most important criteria that are considered as tools to increase the potentiality of the uranium mineralization based on the alteration maps of the different plutons were clarified (Shalaby et al. 2010).

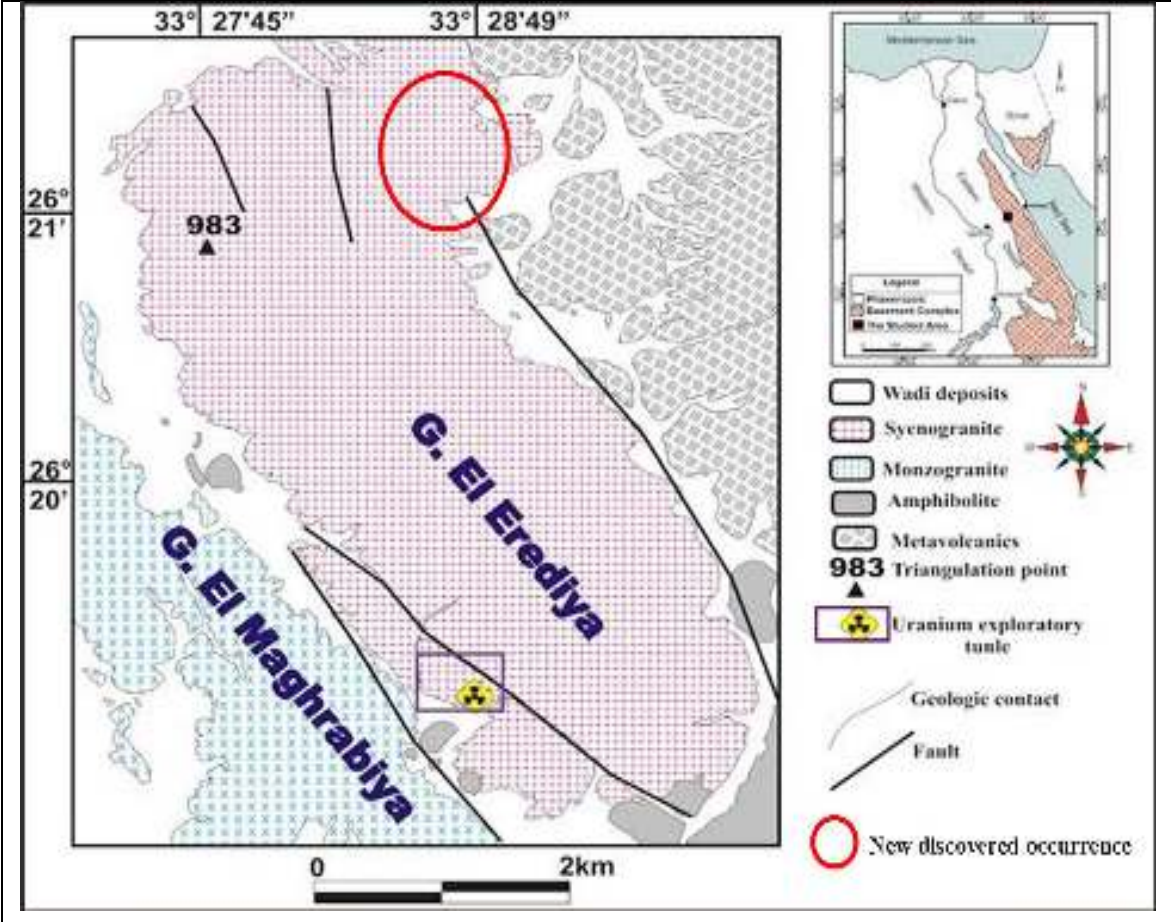


Fig.2: Geologic map of El- Erediya pluton Central Eastern Desert, Egypt (Modified after Omran et. al., 2014).

	
<p>Fig.3a. Close-up view showing hematitization at El-Erediya granite.</p>	<p>Fig.3b. Close-up view showing kaolinization at El-Erediya granite.</p>
	
<p>Fig.3c. Close-up view showing illitization at El-Missikat granite.</p>	

3. Remote Sensing

3.1. Image preprocessing

3.1.1. Crosstalk correction

The original ASTER (Level 1B) scene data were initially corrected for crosstalk effects using the automated Crosstalk Correction Software (ERSDAC, 2001). This crosstalk effect is due to the dispersion of incident light in band 4, which is diffused to the focal plane of other SWIR bands, causing the appearance of noise and related anomalies at the interface of land and water (Iwasaki & Tonooka, 2005).

The existence of possible vertical scaling anomalies in ASTER data and SWIR crosstalk from band 5 and band 9 makes the data difficult to use for spectral analysis based on direct comparisons with library or field spectra (NASA ASTER, 2004). Conducting further rigorous radiometric corrections to the ASTER data in order to obtain surface reflectance and radiance is also not feasible because the information about the atmospheric properties above the study area at the time the ASTER data were collected (such as barometric pressure, relative humidity, and visibility) are not available.

3.1.2 Atmosphere correction

The nature of remote sensing requires that solar radiation pass through the atmosphere before it is collected by the instrument. Because of this, the data must be subjected to atmospherically correction using the Fast Line-of-sight Atmospheric Analysis of Spectral Hypercubes (FLAASH) which involved in ENVI software. With the Atmospheric Correction Module, we can accurately compensate for atmospheric effects and produce an estimate of the true surface reflectance.

3.2 Remote sensing analysis

The ASTER data used in this study are cloud free level 1B data acquired on October 07, 2007. The image has been pre-georeferenced to UTM Zone 36 North projection with WGS-84 datum. The ASTER image was then re-sampled so that VNIR and SWIR bands have the same 15 x 15 m pixel size and then clipped and masked to the granite of El-Erediya.

ASTER is a multi-spectral imaging sensor that measure reflected and emitted electromagnetic radiation from Earth's surface and atmosphere in 14 bands. The spectral bands include: three visible and near infrared radiation (VNIR) bands ranging between 0.52 and 0.86 μm with a spatial resolution of 15 m six shortwave infrared radiation (SWIR) bands from 1.6 to 2.43 μm with a spatial resolution of 30 m and five recording thermal infrared radiation (TIR) bands in the 8.125-11.651 m wave length region with spatial resolution of 90 m. An additional backward looking band in the visible and near infrared radiation makes it possible to construct Digital Elevation Models (DEM) from the nadir view band 3N and back view band 3B. ASTER swath width is 60 km (each scene is 60x60 km) which makes it useful for regional mapping (Abrams, 2000 and Yamaguchi et al., 1998).

To examine the potential of the (ASTER) data in mapping the alteration zones that could host uranium mineralization within the younger granite of El-Erediya pluton, target detection using spectral-matching algorithm was applied to recognize the most predominant alteration components such as hematite, kaolinite, illite and alunite as targets that more or less considered as path finder of uranium mineralization. This led to trace the most promising zones affected by these alterations within the granite of El-Erediya pluton and succeed in mapping and recognize the zones that containing more than one target (co-target) and delineate the promising areas for uranium prospection.

Generally, the target detection is used to locate objects within an image that match the spectral signatures of target minerals. This technique uses a variety of target detection algorithms to search for targets and produce the rule images for each target minerals. The spectra of diagnostic alteration minerals were re-sampled from the spectral library of ASTER using ENVI's software after the targets are detected, the workflow will guide through combining the rule images from each target detection algorithm into a single detection overlay for each target.

The target signature in our study derived from a jpl beckman mineral spectral library of reflectance spectra, of ASTER that involved in ENVI 5.2 software. The spectral signatures of the multi targets (alunite, hematite, illite and kaolinite) are chosen from this spectral library as a known target to detect them within the image of El-Erediya pluton.

If we will assume that an example target spectrum is known and that the image and the target spectrum have been transformed into a common space, the most common target detection algorithm based on a stochastic description of the data is the spectral matched filter in the presence of noise (clutter). Matched filter processing was applied to analyze the ASTER data. The matched filter is a partial spectral unmixing technique that aims to detect the known spectral class of interest while suppressing the background. It is expressed as:

$$MF(x) = \frac{(t - m)^T S^{-1} (x - m)}{\sqrt{(t - m)^T S^{-1} (t - m)}} \quad \begin{matrix} \geq \eta \Rightarrow \text{target} \\ < \eta \Rightarrow \text{no target} \end{matrix}$$

Where t is the target vector, x is the sample vector, m is the background mean and S is the background covariance (Schott, 2007). The resulting $MF(x)$ at η is the thresholded to control the false alarm rate.

In the spectral remote sensing case, the variability is usually dominated by scene variation, not noise, and so we are more appropriately seeking to maximize the signal-to-clutter ratio (SCR). Thus, m and S are the mean of the background (clutter) and the covariance matrix of the background, which includes variation due to scene variability and noise.

To intuitively understand the spectral matched filter (SMF), it is often easier to think of the previous equation as a two-step process. The first step transforms the demeaned target vector and image data into a space that is normalized or whitened by the square root of the background

covariance matrix. This is followed by a projection of the whitened image vector onto the whitened target vector (Schott, 2007). This can be expressed as

$$S^{-1/2}(x - \mu) S^{-1/2} S^{-1/2}(y - \mu) = \left[S^{-1/2}(x - \mu) \right]^T S^{-1/2}(y - \mu) \quad \begin{matrix} \text{is the target} \\ \text{is the target} \end{matrix}$$

A matched filtering algorithm technique was used to detect significant altered minerals using the ASTER VNIR and SWIR surface reflectance data and reference spectra from the ASTER spectral library.

The target detection results, using matched filtering technique, show that the ASTER data were capable of mapping different types of alterations and produce rule images for all minerals that could be associated with the granitic rock of El-Erediya pluton. The ASTER-derived alteration zones show excellent correlation with that on field and on the reference geologic map.

A group of alteration, locally the most favorable associated to uranium mineralization was mapped with the ASTER data and more importantly to the uranium exploration. These alterations were mapped in some areas that were not shown on the previous geologic map.

Density Slice Technique was carried out by conversion of raster grey scale image of product rules to vector file. Transform the highly brightness pixels of the product rule that corresponding and mapped areas of highly alteration into areas represented by red, green, yellow and blue color for the hematite, alunite, kaolinite and illite respectively with a Producer's accuracy of more than 68%, (Figs. 4a, b, c and d).

This work also succeed in mapping and recognize the zones that containing more than one target (co-target) and delineate the promising areas for uranium prospection which marked by the red circles (Fig.4e). Although one of these promising zones (the southern one) considered as the preexistence prospect area, the other two promising zones are became new areas for detail and further prospection.

		
<p>Fig.4a. Matched filtering rule image of hematitization.</p>	<p>Fig.4b. Matched filtering rule image of alunization.</p>	<p>Fig.4c. Matched filtering rule image of kaolinization.</p>
		
<p>Fig.4d. Matched filtering rule image of illitization.</p>	<p>Fig. 4e. Co-target image showing the promising zones</p>	

4. Result

The field works and the radiometric investigations revealed that the gamma radioactivity of the all altered zones is relatively high. Only one location from the previously mentioned tow locations at the North Eastern part of El Erediya pluton (Fig. 4e) is discovered as high radioactive anomalies with some uranium mineralizations, mainly confined to the alteration zones within the younger granites, while the other one could not subjected to detailed investigations due to the rugged topography of their host rocks. The newly discovered high radioactive anomalies and uranium mineralized zones are located at the northeastern parts of El Erediya pluton.

Representative samples were selected from the newly discovered highly radioactive and mineralized part for the purpose of mineralogical studies and mineral identification. Conventional mineralogical investigation methods and techniques were carried out, including: crushing, sieving, washing, drying, separation and purification with heavy liquid in order to obtain pure mono-mineralic fractions. The obtained uranium minerals and their association are identified using different techniques such as binocular and reflected light microscope and x-ray diffraction for both the separated grains. Moreover, the using of scanning electron microscope (SEM) for the selected grains while using the elemental x-ray detector namely as EDX (Energy Dispersive X-ray) spectrometer give both qualitative and quantitative information about the scanned minerals.

The alteration features connected with this mineralized zone are predominantly hematitization (Fig.5a), silicification with jasper vein (Fig.5b) and often accompanied by kaolinitization (Fig.5c), carbonitization and chlortization. Most of these alterations are generally of hydrothermal nature and their distribution is structurally controlled.

Hydrothermal minerals have a distinct distribution pattern in different types of hydrothermal systems characterized by groups of minerals that have spectral features in the near-and middle-infrared. These spectral features are the result of electronic and vibration processes (Hunt, 1977 and 1979).



Fig.5a. Close-up view showing slightly hematitized part of the anomalous zone.



Fig.5b. Close-up view showing jasperoid vein associated with the anomalous zone



Fig.5c. Close-up view showing the anomalous zone stained by kaolinite and hematite alteration

4.1 Mineralogical Studies

The studied samples were characterized by the mineral assemblage including: uranophane, fluorite and zircon.

4.1.1. Uranophane $[\text{Ca} (\text{UO}_3)_2 (\text{SiO}_3)_2 (\text{OH})_2 \cdot 5\text{H}_2\text{O}]$

Uranophane represents the most abundant radioactive minerals in the new radioactive zone within El-Eredyia pluton and exhibits different grades of canary to yellow color. It mostly occurs as divergent clusters of prismatic to acicular grains, but few grains occur as anhedral massive crystals. X-ray diffraction analyses are in accordance with ASTM card (8-442) of uranophane. SEM -EDX analyses of some uranophane mineral grains reveal that the mineral is composed essentially of U (about 80%), Ca and Si, with traces of Al, K and Fe (Fig.6a).

4.1.2. Fluorite [CaF₂]

Fluorite commonly occurs in hydrothermal, pegmatitic and pneumatolytic veins, in greisens and in cavities in granites. In the studied new occurrence of El-Erediyia pluton, fluorite occurs as anhedral to subhedral irregular fragments of vitreous luster. The color of this mineral range from purple, violet, blue and deep blue colors (Fig.6b). The coloration of fluorite may be due to the presence of radioactive materials in or around the fluorite mineral grains. Raslan (1996) concluded that rocks which are rich in secondary uranium minerals are usually rich in fluorite of deep blue to violet colors. From its SEM-EDX analysis the mineral is composed essentially of Ca and F with the presence of trace amounts of U, Si, P and Al.

4.1.3. Zircon [ZrSiO₄]

Zircon is generally found as colorless grains, in some cases found in color state. Zircon is transparent and prismatic shape with bipyramidal termination. Zircon is found in two states, the normal zircon and metamict one. Metamictization of zircon is due to the presence of radioactive atoms (Deer et al., 1966). SEM-EDX analyses of some zircon mineral grains reveal that the mineral is composed essentially of Zr and Si (Fig.6c).

5. Conclusion

In conclusion, the image processing methods used can provide cost-effective information to discover possible locations of uranium mineralization prior to detailed and costly ground investigations. The extraction of spectral information from ASTER data can produce comprehensive and accurate information for resource investigations around the world. El-Erediyia pluton represents one of the most important prospect areas in the Central Eastern Desert which comprise different types of alteration with U-mineralization confined to the El-Erediyia granites. Recognition of hydrothermally altered rocks associated with uranium mineral was carried out using image processing techniques such as target detection and matched filtering. These techniques led to recognized of three target zones each one contain more than one alteration within the studied granites. Extensive geological and radiometric investigations were carried out for the alteration zones, delineated by the ASTER image processing. During the field works, the radiometric investigations revealed that the gamma radioactivity of the all altered zones is relatively high. The only one location is discovered high radioactive anomaly with some uranium mineralizations, mainly connected to the extensively altered zones within El Erediyia granites, while the other zone could not subjected to detailed investigations due to the rugged topography of their host rocks.

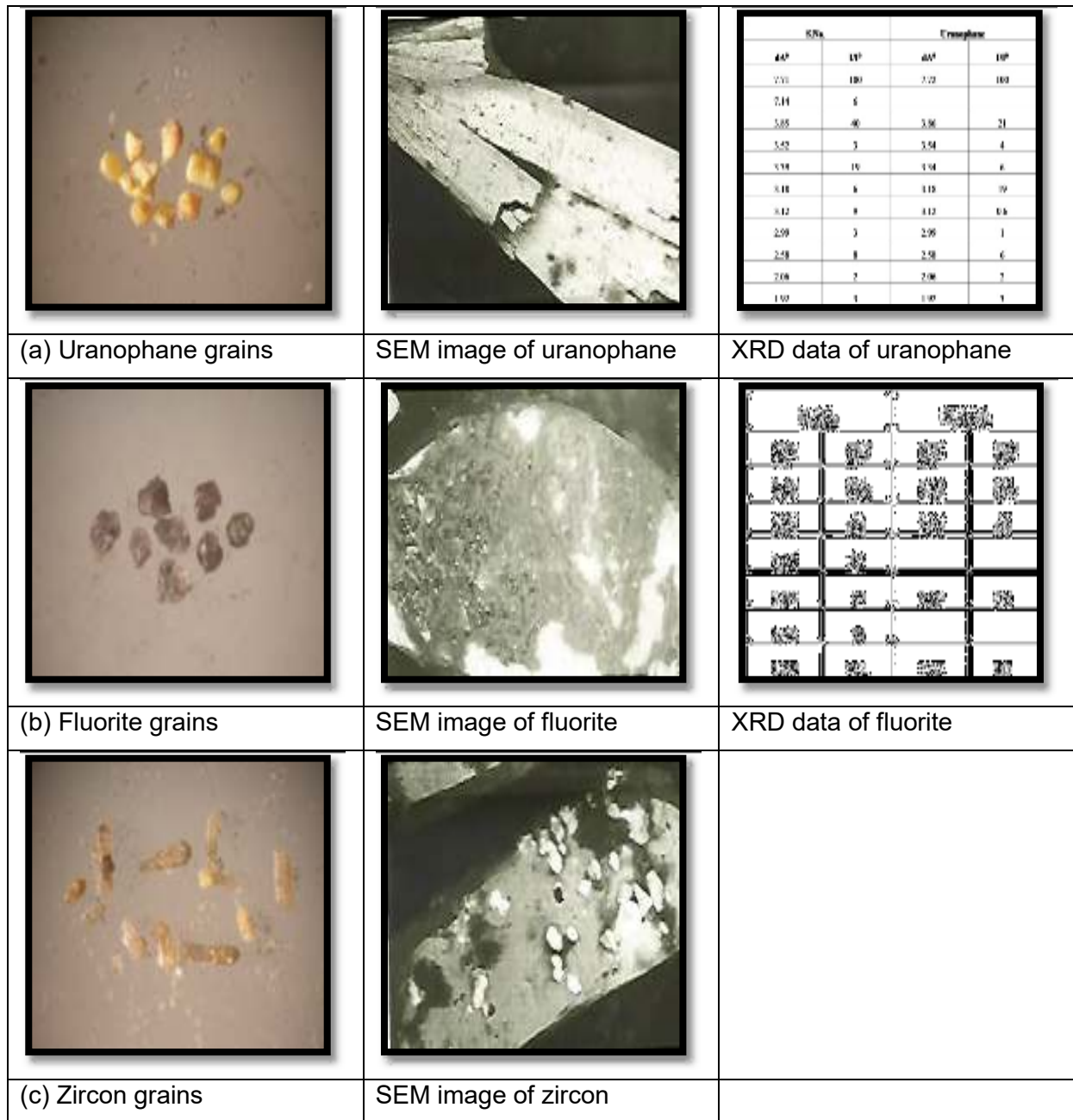


Fig. 6: Showing Stereophotomicrographs of the most important heavy minerals (a) uranophane, (b) fluorite and (c) zircon and their SEM image and XRD data respectively.

References

- Abd El-Naby, H.H., (2007):** Genesis of secondary uranium minerals associated with jasperoid veins, El Erediya area, Eastern Desert, Egypt. *Miner Deposita* 43, 933-944.
- Abrams, M.J., (2000):** The advanced spaceborne thermal emission and reflection radiometer (ASTER): data products for the high spatial resolution imager on NASA's Terra platform. *International Journal of Remote Sensing* 21, 847–859.
- Abu Dief, A., (1992):** The relation between the uranium mineralization and tectonics in some Pan-African granites, west of Safaga, Eastern Desert, Egypt. Ph.D. Thesis, Assiut Univ., Egypt, 218 p.
- Aero-Service, (1984):** Final operational report of airborne magnetic/radiation survey in the Eastern Desert, Egypt for the Egyptian General Petroleum Corporation. Aero Service, Houston, Texas.
- Amer, R., Kusky, T.M., Ghulam, A., (2010):** New methods of processing ASTER data for lithological mapping: examples from Fawakhir, Central Eastern Desert of Egypt. *J. Afr. Earth Sci.* 56 (2–3), 75–82
- Ammar, A. A., (1973):** Application of aerial radiometry to the study of the geology of Wadi El Gidami, Eastern Desert (with aeromagnetic application). Ph. D. Thesis, Faculty of Science, Cairo University, 424.p.
- Attawiya, M.Y. (1983):** Mineralogical study of El Erediya-I Uranium occurrence. Eastern Desert, Egypt: *Arab Oour. Nucl. Sc. Techn.* V;16, No.2, pp. 221-236.
- Azizi, H., Tarverdi, M.A., Akbarpour, A., (2010):** Extraction of hydrothermal alterations from ASTER SWIR data from east Zanjan, northern Iran. *Adv. Space Res.* 46 (1), 99–109.
- Bakhite, F. S., (1978):** Geology and radioactive mineralization of G. El-Missikat area, Eastern Desert, Egypt. Ph.D Thesis, Ain Shams University, Cairo, Egypt, 289p.
- Bedini, E., (2011):** Mineral mapping in the Kap Simpson complex, central East Greenland, using HyMap and ASTER remote sensing data. *Adv. Space Res.* 47, 60–73 .
- Deer, W. A., Howie, R. A. and Zussman, J., (1966):** An introduction to rock forming minerals. Longmans, London. P517.
- Di Tommaso, I., Rubinstein, N., (2007):** Hydrothermal alteration mapping using ASTER data in the In fiernillo porphyry deposit, Argentina. *Ore Geol. Rev.* 32, 275 –290.
- Ducart, D. F., Crosta, A . P., Souza, C. R., & Coniclio, J. (2006):** Alteration mineralogy at the Cerro La Mina epithermal prospect, Patagonia, Argentina: Field mapping, shortwave infrared spectroscopy, and ASTER images. *Economic Geology*, 101, 981 – 996.
- El-Kassas, I. A. (1974):** Radioactivity and geology of Wadi Atalla area, Eastern Desert of Egypt. Ph.D. Thesis, Faculty of Science, Ain Shams University, Cairo, Egypt, 502 p.
- ERSDAC -Earth remote sensing data analysis center (2001):** The crosstalk correction software: User's guide.: Mitsubishi Space Software Co. Ltd. 17 pp.
- Fullagar, P. D., (1980):** Pan-African age granites of North Eastern Africa: New or reworked sialic materials, in Salem, M. J. and M. T. Busrewil, eds., *Geology of Lybia, Second symposium in the geology of Lybia*, v. 3: New York, Academic press, P. 1050-1058.
- Gabr, S., Ghulam, A., Kusky, T., (2010):** Detecting areas of high-potential gold mineralization using ASTER data. *Ore Geol. Rev.* 38, 59–69
- Hellman, M. J., & Ramsey, M. S. (2004):** Analysis of hot springs and associated deposits in Yellowstone National Park using ASTER and AVIRIS remote sensing. *Journal of Volcanology and Geothermal Research*, 135, 195 – 219.
- Hubbard, B. E., & Crowley, J. K. (2005):** Mineral mapping on the Chilean-Bolivian Altiplano using co-orbital ALI, ASTER and Hyperion imagery: Data dimensionality issues and solutions. *Remote Sensing of Environment*, 99, 173– 186.
- Hunt, G.R., (1977):** Spectral signatures of particulate minerals, in the visible and near-infrared. *Geophysics* 42, 501-513.
- Hunt, G.R., Ashley, P., (1979):** Spectra of altered rocks in the visible and near infrared. *Ecol. Geol.*

El Zalaky & Abdelmonsif. The Arab Journal of Sciences & Research Publishing, Vol. 2 - Issue (3): 2016, 4, 21 P. 120-133; Article no: AJSRP/ Z15216.

74, 1613-1629.

Hussein, H. A., (1987): *Geochemistry of granitic rocks and uranium mineralization in El-Missikat - El-Erediya area, SW Safaga, Eastern Desert, Egypt. Ph.D. Thesis, Faculty of Science, Cairo Univ., 215 p*

Iwasaki, A., & Tonooka, H. (2005): *Validation of a crosstalk correction algorithm for ASTER/SIWR. IEEE Transactions on Geoscience and Remote Sensing, 43, 2747–2751.*

Kamel, A.I., (1998): *Stress field controlling joint-type U-mineralization in some granitic plutons in the Central Eastern Desert of Egypt. Ph. D. Cairo Univ., p. 253.*

NASA ASTER,(2004): *Advanced Spaceborne Thermal Emission and Reflection Radiometer. Available from: <<http://asterweb.jpl.nasa.gov>>.*

Mohamed, N. A., (1988): *Mineralogical and petrographical characteristics of some alteration products related to uranium mineralization in El-Missikat- El-Erediya areas, Eastern Desert, Egypt. M.Sc. Thesis, Faculty of Science, Cairo Univ., 118 p.*

Omran, A., Abdallah. S., Abd-El Monsif. M., El-Desoky. O., Hamed. A., Arbab. A. and Ahmed. A.(2014): *El Missikat-El Erediya uranium development project. El Erediya area. Int. report.*

Osmond, J. K., Dabous, A. A. and Dawood, Y. H., (1999): *Uranium series age and origin of two secondary uranium deposits, Central Eastern Desert, Egypt. Econ. Geol., Vol. 94, pp. 273 - 280.*

Pour, B.A., Hashim, M. (2011a): *Identification of hydrothermal alteration minerals for exploring of porphyry copper deposit using ASTER data, SE Iran. J. Asian Earth Sci. 42, 1309–1323, 2011a.*

Rabie, S. I. and Ammar, A. A., (1990): *Delineation of geological structures from aero-magnetic data using some integrated interpretation techniques, El-Missikat and El-Erediya granitic plutons, Central Eastern Desert, Egypt. E.G.S. 8 th Ann. Meet., "March, 1990", pp. 111 - 134.*

Raslan, M. F., (1996): *Mineralogical and beneficiation for some radioactive granites along Wadi Balih, North Eastern Desert, Egypt. M.Sc.thesis. Faculty of Science, Cairo Univ., p183.*

Rockwell, B. W., & Hofstra, A. H. (2008): *Identification of quartz and carbonate minerals across northern Nevada using ASTER thermal infrared emissivity data Implications for geologic mapping and mineral resource investigations in well-studied and frontier areas. Geosphere, 4,218–24 6.*

Rowan, L. C., Hook , S. J., Abrams, M. J., & Mars, J. C. (2003): *A new satellite imaging system for mapping hydrothermally altered rocks: An example from the Cuprite, Nevada Mining District USA. Economic Geology Bulletin , 98 ,1019– 10 2 7.*

Sabins, F.F., (1999): *Remote sensing for mineral exploration. Ore Geol. Rev. 14, 157– 183.*

Schott, J.R. (2007): *Remote sensing. The Image Chain Approach. second ed. Oxford University Press, New York, p. 688,.*

Shalaby, H. M., Bishta, Z. A., Roz, M. E. and El Zalaky, M. A. (2010): *Integration of Geologic and Remote Sensing Studies for the Discovery of Uranium Mineralization in Some Granite Plutons, Eastern Desert, Egypt. JAKU: Earth Sci., Vol. 21, No. 1, pp: 1-25.*

Vaughan, R. G., Hook , S. J., Calvin, W. M., & Taranik, J. V. (2005): *Surface mineral mapping at Steamboat Springs, Nevada, USA, with multi-wavelength thermal infrared images. Remote Sensing of Environment, 99, 140-158.*

Vaughan, R. G., Kervyn, M., Realmuto, V. J., Abrams, M. J., & Hook , S. J. (2008): *Satellite thermal infrared measurements of recent volcanic activity at Oldoinyo Lengai, Tanzania. Journal of Volcanology and Geothermal Research, 173, 196- 206.*

Yamaguchi, Y., Kahle, A., Tsu, H., Kawakami, T., Pniel, M., (1998): *Overview of advanced thermal emission and reflection radiometer (ASTER). IEEE Transactions on Geoscience and Remote Sensing 36, 1062e1071.*

Zhang, X., Pamer, M., & Duke, N. (2007): *Lithologic and mineral information extraction for gold exploration using ASTER data in the South Chocolate Mountains (California). ISPRS Journal of Photogrammetry and Remote Sensing, 62, 271-282.*